# RISING OF A BUBBLE IN AN UPWARD FLUID FLOW IN A VERTICAL PIPE

P. K. Volkov

UDC 532.529.6

In modern heat exchangers, pipes, and capillaries there occurs motion of liquid which contains bubbles of dissolved gases or vapor of different size. The forced motion of fluid (pumping) is produced either by creating a pressure difference at the ends of the pipe or with the help of pumps. In the first case it is said that the flow occurs with a given pressure drop (the flow rate is unknown and is a paremeter to be determined) while in the second case the flow occurs with a given flow rate (the pressure drop must be found by solving the problem). From the mathematical standpoint, these two formulations are, as a rule, equivalent in the sense that if the problem with the fixed flow rate has been solved, then the presure drop can be calculated, and if the problem with the determined pressure drop is solved, then the starting flow rate is obtained [1].

The theoretical investigation of the local characteristics of a liquid moving in a pipe with gas bubbles rising upward presents significant difficulties owing to the fact that the flow has a free surface which is not known beforehand and which must be determined together with the flow functions. There are very few experimental data [2-4] and they give only a qualitative idea of the process. Since the problem contains more than three independent input parameters, the results of the experiments cannot be generalized at the present time. Probably only a numerical solution of the Navier–Stokes equations will make it possible to give a complete picture of flow near a deformable bubble. An algorithm for solving numerically the complete Naver–Stokes equations describing the rising of a gas bubble in a vertical pipe filled with a fluid at rest is given in [5]. Analysis of the solutions obtained and a map of the flow regimes for a wide range of input parameters are given in [6]. In this paper the results of calculations of stationary rising of a bubble in a liquid in which far from from the bubble the velocity profile over the cross section of the pipe is parabolic are presented.

1. Formulation of the Problem. Consider a vertical pipe filled with a viscous liquid moving upward. The acceleration due to gravity g is directerd downwards. If a gas bubble is introduced into the pipe, then it will rise under the action of the buoyancy force and it will be carried by the flow of moving liquid. If the volume, shape, and velocity of the bubble does not change much on some section of its path, then we regard the rising of the bubble to be stationary. In a coordinate system attached to the walls of the pipe, the rise velocity u is obviously higher than the rise velocity $u_0$ of a bubble in a fluid at rest and depends on the flow rate of the pumped liquid around the bubbble and the shape of the bubble. We assume that far from the bubble a Poiseuille flow, characterized by one parameter, for example, the maximum velocity $u_n$ on the axis, is established above and below the bubble in the pipe.

It is convenient to give the mathematical description in a coordinate system tied to the bubble. Then the bubble is at rest and the walls of the pipe and the liquid move downward (Fig.1). In a spherical coordinate system $(r, \theta, \varphi)$ whose origin O lies at the "center of the bubble" the motion of the liquid is descrbed by the Navier–Stokes equations, and owing to the axial symmetry, in the terms the stream function $\psi$ – the vorticity $\omega$ assumes the form [6]

$$D^2\psi = -2r\sin\theta\,\omega; \tag{1.1}$$

$$D^2\omega = \frac{1}{\nu r^2\sin\theta}\left[\psi_\theta\omega_r - \psi_r\omega_\theta - \frac{\omega}{r}\psi_\theta + \omega\operatorname{ctg}\theta\psi_r\right] - \frac{2}{r}\omega_r + \frac{\omega}{r^2\sin^2\theta} - \frac{2\operatorname{ctg}\theta}{r^2}\omega_\theta \tag{1.2}$$

$$\left(D^2 \equiv \frac{\partial^2}{\partial r^2} + \frac{\sin\theta}{r^2}\frac{\partial}{\partial\theta}\left(\frac{1}{\sin\theta}\frac{\partial}{\partial\theta}\right)\right).$$

Novosibirsk. Translated from Zhurnal Prikladnoi Mekhaniki i Tekhnicheskoi Fiziki, No. 4, pp. 35-42, July-August, 1991. Original article submitted March 28, 1989; revision submitted April 26, 1990.

 0021-8944/91/3204-0496$12.50 

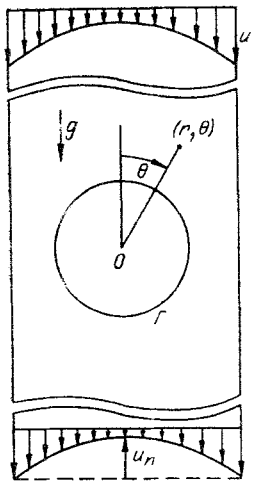


Fig. 1

We prescribe the boundary conditions as follows: a) on the surface of the bubble $\Gamma(r = R(\theta), \theta \in [0,\pi])$ we impose the condition of impenetrability, the tangential stresses are equal to zero, and the difference of the normal stresses is equal to the capillary forces:

$$\psi(r, \theta) = 0; \tag{1.3}$$

$$\omega + \frac{R^2 + 2R'^2 - RR''}{R^2 + R'^2} \frac{\psi_r}{r^2 \sin\theta} = 0; \tag{1.4}$$

$$-p(r, \theta) + 2\rho\nu \left[ \frac{\psi_{\theta r} - \psi_\theta / r + R'\psi_{rr}}{r^2 \sin\theta} + \frac{R'}{R}\omega \right] = -p_g + \sigma K \tag{1.5}$$

$\left[K = \frac{R^2 + 2R'^2 - RR''}{(R^2 + R'^2)^{3/2}} + \frac{|R'\cos\theta - R\sin\theta|}{R\sin\theta\,(R^2 + R'^2)^{1/2}}\right.$ is the curvature $\Gamma$, $\nu$ is the coefficient of kinematic viscosity, $\sigma$ is the surface tension, $p = q - \rho g r \cos\theta + p_\infty$ ($p_\infty = p(r = R_p, \theta = \pi/2)$) is the pressure in the liquid, q is the generalized pressure, $p_g$ is the pressure of the gas in the bubble (assumed to be constant), and $\rho$ is the density of the fluid];

b) on the pipe walls ($r = G(\theta)$, $\theta \in [\theta^*, \pi - \theta^*]$, $\theta^* = \arctan(R_p/\ell)$, $R_p$ is the radius of the pipe, and $2\ell$ is the length of the selected section of the moving pipe) we impose the no-slip and impenetrability conditions:

$$\frac{1}{r}\frac{\partial\psi}{\partial r} + \frac{\cos\theta}{r^2\sin\theta}\frac{\partial\psi}{\partial\theta} = -u; \tag{1.6}$$

$$\psi(r, \theta) = -\frac{u}{2}R_p^2\left(1 - \frac{u_n}{2u}\right); \tag{1.7}$$

c) on the axis of the pipe ($\theta = 0, \pi$) we impose the symmetry condition

$$\psi(r, \theta) = \omega(r, \theta) = 0; \tag{1.8}$$

d) at the inlet ($r = F_1(\theta)$, $\theta \in [0, \theta^*]$) and the outlet ($r = F_2(\theta)$, $\theta \in [\pi - \theta^*, \pi]$)

$$\psi(r, \theta) = -\frac{u}{2}r^2\sin^2\theta + \frac{u_n}{2}r^2\sin^2\theta\left(1 - \frac{r^2\sin^2\theta}{2R_p^2}\right); \tag{1.9}$$

$$\omega(r, \theta) = u_n r \sin\theta / R_p^2. \tag{1.10}$$

Equations (1.7), (1.9), and (1.10) contain terms which are associated with the Poiseuille flow in the pipe. Thus, if the fluid is not pumped ($u_n = 0$), we have the conditions [6] corresponding to undisturbed flow. If $u_n > 0$, additional flow appears in the pipe cross sections; this is taken into account in Eq. (1.7). At the inlet and outlet of the pipe we prescribe a Poiseuille parabola: $V(y) = u_n(1 - y^2/R_p^2)$ (y is the coordinate measured across the pipe). Then the radial component of the velocity is

$$u_r = \frac{1}{r^2 \sin\theta}\frac{\partial\psi}{\partial\theta} = u_n\left(1 - \frac{r^2\sin^2\theta}{R_p^2}\right)\cos\theta$$

or $\partial\psi/\partial\theta = u_n r^2 \sin\theta\cos\theta(1 - r^2\sin^2\theta/R_p^2)$. Integrating over $\theta$ with r = const we obtain $\psi(r, \theta) = u_n[(r^2\sin^2\theta)/2][1 - (r^2\sin^2\theta)/2R_p^2]$. Substituting now $\psi(r, \theta)$ into Eq. (1.1) we calculate $\omega(r, \theta)$ at the inlet and outlet of the pipe (1.10). The parameter $u_n$ is an independent parameter and determines the flow rate of the liquid pumped through the cross section of the pipe. For large values of $R_p$ and a small bubble the rise velocity of the bubble is equal to the sum of the rise velocity in the fluid at rest $u_0$ and $u_n$. As the pipe diameter decreases u will now be determined by the entire flow pattern.

2. Dimensional Analysis and Method of Solution. The problem (1.1)-(1.10) contains the following dimensional imput parameters: $\rho$, $\nu$, $\sigma$, g, $p_g - p_\infty$, $R_p$, and $u_n$. The size, shape, and rise velocity of the bubble and the flow functions are found by solving Eqs. (1.1)-(1.10). According to the theory of dimensional analysis, the problem (1.1)-(1.10) has four dimensionless independent combinations. If $a$ (the radius of a sphere with an in equivalent volume) and u are taken as the characteristic size and velocity and the equations are made dimensionless [5], then the equations of motion and the boundary conditions will contain the following parameters: the Reynolds number $Re = u2a/\nu$, Weber's number $We = \rho u^2 2a/\sigma$, Froude's number $Fr = u^2/ga$, and pressure difference $p_d = (p_g - p_\infty)/\rho u^2$, the pumping velocity $W = u_n/u$, and $\lambda = a/R_p$, which characterizes the geometry of the flow region. Four of the six indicated dimensionless combinations must be independent. If Re and We are assumed to be given, then Fr and $p_d$ cannot be prescribed beforehand and they must be determined together with the flow functions, for example, as done in [6].

The problem (1.1)-(1.10) differs from the problem solved in [6] in that the conditions (1.7), (1.9), and (1.10), which prescribe the flow rate of the liquid, are different and the flow at the inlet and outlet of the pipe is a Poiseuille flow instead of a uniform flow. For this reason, the method of solution and algorithm will be analogous. The problem is solved for each value of $\lambda$, fixed W, and different values of Re and We. Then by changing W we can obtain an extremely large amount of information about the flows. The existence of four independent dimensionless parameters makes it virtually impossible to investigate completely the problem formulated. For this reason, in this work we shall confine our attention to the most interesting and important case, when the bubble size is comparable to the pipe size. Indeed, if we have a growing vapor bubble, which is rising in the pipe, then as long as the bubble is small no significant features appear in the flow. But when the bubble starts to occupy a large fraction of the cross section of the pipe, then the deformation of the surface brings about a substantial decrease of the rise velocity of the bubble [6]. Thus, for $\lambda = 0.8$ and 0.98 calculations were performed for W = 0.5 and 1. With the help of the data in [6] (corresponding to W = 0) the characteristic flow features owing to the pumped liquid can be determined. The analysis is performed and the results are represented by constructing diagrams of isolines of Fr in the coordinates $R_\sigma = a/(\sigma/\rho g)^{1/2}$, $R_\nu = a/(\nu^2/g)^{1/3}$ [6]; the basic types of flows are indicated in these diagrams. In the coordinates employed here each liquid is represented by the straight line whose slope is determined by Morton's number $M = g\nu^4\rho^3/\sigma^3 = (R_\sigma/R_\nu)^6$. Thus, by constructing the lines Fr = const in these coordinates we have complete information about the flow: The rise velocity of the bubble and the flow rate of the pumped liquid, which are easily calculated from Fr and W for a bubble a fixed size $a$ in a specific liquid.

3. Strong Effect of the Walls ($\lambda = 0.8$). We performed a series of calculations for W = 0.5 and different values of Re and We. Even when the bubble is located at a distance of 1-1.5 units from the pipe the fluid flow is the same and differs little from the flow prescribed at the inlet and outlet. The flow is stratified with the velocity oriented parallel to the axis of the pipe, except in the region directly adjacent to the bubble. As the liquid flows past the bubble, behind the bubble a current forms along the axis of the pipe and the liquid slows down at the walls of the pipe. However, these processes are not as pronounced as in the case W = 0 [6]. For example, for Re = 100, We = 0.166, $R_\sigma = 0.35$, $R_\nu = 15.4$, and $M \sim 10^{-10}$ the structure of the flow is the same as in Fig. 7a in [6] for Re = 0.4. For smaller values of Re the character of the flow is the same, but with a weaker stagnation zone and stream; for Re = 4 there are virtually no stream and no stagnation zone. Behind the bubble, and in the expanding part of the flow, there is a fan of velocities in the cross section of the pipe; the minimum (nonzero) velocity occurs on the surface of the bubble.

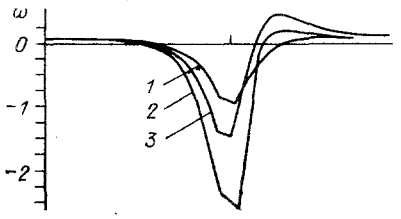


Fig. 2

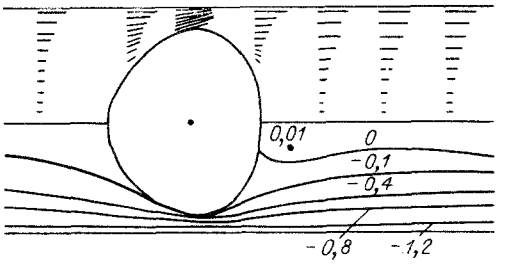


Fig. 3

As We increases with fixed Re the bubble is flattened and the gap between the walls and the pipe decreases. In addition, the velocity distribution near the bubble is even more uniform. Figure 2 shows the distribution of vorticity $\omega$ on the wall of the pipe, when Re, We, and M are equal to, respectively, 4, 0.05, and $2.6 \cdot 10^{-5}$ for the line 1, 40, 0.34, and $2.4 \cdot 10^{-7}$ for the line 2, and 100, 0.166, and $\sim 10^{-10}$ for the line 3. In the region in front of the bubble $\omega$ decreases sharply, indicating that here the liquid accelerates. Immediately behind the narrow part of the gap $\omega$ increases, becomes positive, and then reaches a constant value, corresponding to the Poiseuille flow. Since the friction on the pipe wall $\tau = (2/\mathrm{Re})\omega$, the losses associated with the passage of the bubble can be determined. Comparing the plots in Fig. 2 shows that the peak of vorticity $\omega$ is highest for the curve 2. This is explained by the fact that the curves 1 and 3 correspond to virtually spherical bubbles with the same distance between the bubble and the pipe wall in the narrow gap. Curve 2 corresponds to a flattened bubble, when the gap has significantly decreased. Since the flow rate in the pipe is fixed, this leads to higher fluid velocity in the gap and therefore sharply reduced vorticity $\omega$. Comparing the computed values of Fr at the corresponding points of the diagram in Fig. 6 from [6] shows that in the region of spherical bubbles Fr increased approximately by a factor of 2.5, while in the region of deformed bubbles it increased by less than a factor of two. Since $\mathrm{Fr} = u^2/ga$, forming the ratio of the Froude numbers and taking its square root we obtain an esimate of the increase in u as compared with the process in a fluid at rest. In the case at hand weakly deformed bubbles rise $\sqrt{2.5}$ times faster than in a fluid at rest. The rise velocity for deformed bubbles is somewhat lower than the sum of the rise velocities in a fluid at rest and the average flow rate at the inlet. For spherical bubbles a linear dependence $\mathrm{Fr} = k_1\mathrm{Re}$ ($k_1 = 0.0095$) is observed.

As the amount of liquid pumped through the pipe increases the structure of the entire flow changes substantially and becomes increasingly less like the pattern observed with a bubble rising in a fluid at rest. The bubble begins to act like a piston, pushing the liquid. Figure 3 shows the flow for Re = 40, We = 0.96, $M = 2.38 \cdot 10^{-6}$, $R_\sigma = 1.22$, $R_\nu = 11.1$, W = 1. Behind (and in front of) the bubble there forms on the axis of the pipe a structure corresponding to the flow behind a piston. For large values of Re the structure does not touch the bubble. This is a result of the virtually vanishing stream of liquid behind the bubble, as one can see from Fig. 7 in [6]. The vorticity $\omega$ and friction $\tau$ at the pipe wall are of the same character as that shown in Fig. 2. The absolute magnitude of the negative peaks decreased by approximately a factor of two. Calculations for other values of Re and We give a flow pattern that differs from Fig. 3 near the bubble. Figure 4 shows the isolines Fr = const in the coordinate $R_\sigma$, $R_\nu$. Their behavior is analogous to the case of a bubble rising in a liquid at rest [6]. The region I of spherical bubbles (left-hand side, bounded by the solid broken line) practically coincides with the region II of deformed bubbles. To the right of the dashed line deformation occurs by stretching along the axis of the pipe with an increasing gap between the bubble and the pipe walls. The stagnation zone at the pipe wall behind the bubble has almost vanished. The rise velocity is higher. Comparing the values of Fr at the corresponding points of the diagrams Figs. 4 and 6 from [6] shows that in the region I their ratio ≈10-13 while in region II ≈5-7. Thus, spherical bubbles rise approximately 3.5 times faster than in a fluid at rest, while deformed bubbles rise more than two times faster. Taking into account the flow rate of the pumped liquid, we can conclude that for spherical bubbles u is larger than the sum of the rise velocity $u_0$ in the fluid at rest and the average flow velocity $u_a$. Indeed, $u = 3.5\ u_0$. Since W = 1, in dimensional form $u_n = u$ and $u_a = u_n/2 = 1.75\ u_0$. Then $u_0 + u_a = 2.75\ u_0 < u$. For deformed bubbles u is approximately equal to (somewhat larger than) $u_a + u_0$. In the region of spherical bubbles $\mathrm{Fr} = k_2\mathrm{Re}$ ($k_2 = 0.0244$).

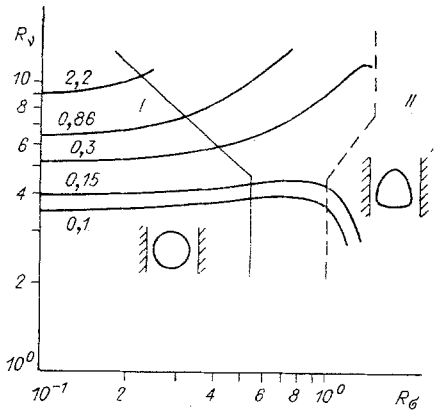


Fig. 4

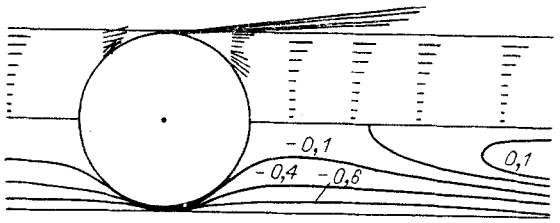


Fig. 5

4. Slug Flow Regime ($\lambda = 0.98$). The term slug here differs from the standard slug regime, when the rise velocity of a bubble no longer depends on its volume for a pipe of the indicated radius. As follows from the diagram in [6], in capillary tubes (whose radius is less than the capillary constant $\delta_\sigma = (\sigma/\rho g)^{1/2}$) in a given liquid the dependence of the rise velocity of a bubble on the bubble volume is nonmonotonic and as the equivalent radius $a$ approaches the pipe radius the rise velocity decreases strongly. This is explained by the fact that in such pipes the surface tension of a bubble is large and predominates over the inertial and viscous forces. The bubble becomes "rigid," remaining virtually undeformed and spherical. As the volume of the bubble increases, the bubble plugs up the capillary. In pipes whose radius $R_p$ is greater than $\delta_\sigma$, as $a$ approaches $R_p$ the inertial forces become comparable to the surface tension force, and bubble is deformed along the axis of the pipe, and the rise velocity of the bubble increases. The presence of upward flow should result in an increase of the rise velocity, whose magnitude will be determined by the shape of the bubble. The flow pattern for $W = 0.5$, $Re = 100$, $We = 0.0008$, $M \sim 10^{-12}$ is reminiscent of the structure with $W = 0$ and $Re = 60$ [6]. Here, however, at the pipe wall behind the bubble there is a stagnation zone without closed stream lines. As We increases the bubble at first becomes flattened, in spite of the small gap, and then (for $R_\sigma > 0.8$) it stretches out along the axis of the pipe and the gap between the pipe and bubble walls increases. For smaller values of Re the flow pattern is on the whole analogous, but the stream behind the bubble and the stagnation zone at the wall are less pronounced. The regions of characteristic types of flows arise, as in [6], and are virtually identical to the diagram for $\lambda = 0.98$. The rise velocity of the bubble is approximately 1.2 times higher than in the case $W = 0$. This means that $u = 1.2\ u_0$. Since $u_a = u_n/2 = 2/4$, we have $u_0 + u_a = u_0 + 0.3\ u_0 > u$. Thus, for $W = 0.5$ the bubbles rise with a velocity higher than $u_0$ but less than $u_a + u_0$. In the region of spherical bubbles $Fr = k_3 Re$ ($k_3 = 0.000035$).

As the flow rate of the liquid pumped through the pipe increases the structure of the flow changes. Figure 5 shows the pattern for $W = 1$, $Re = 100$, $We = 0.0014$, $M \sim 10^{-13}$, $R_\sigma = 0.42$, $R_\nu = 85$. The stream behind the bubble and the stagnation zone at the wall are very insignificant. On the axis of the pipe at some distance from the bubble there forms a structure corresponding to the fluid flow behind a piston. For smaller values of Re the zero stream line is closed on the bubble. Figure 6 shows plots of the vorticity $\omega$ at the pipe wall for $W = 1$ for the case when Re, We, M, $R_\sigma$, and $R_\nu$ take on the following values, respectively: for the line 1) 4, 0.0016, $4.6 \cdot 10^{-8}$, 1.07, 17.8; for the line 2) 40, 0.0054, $\sim 10^{-11}$, 0.93, and 50.1; for the line 3) 100, 0.0014, $\sim 10^{-13}$, 0.42, and 85. The negative peaks of $\omega$ are approximately two times smaller than those with the corresponding values of the parameters

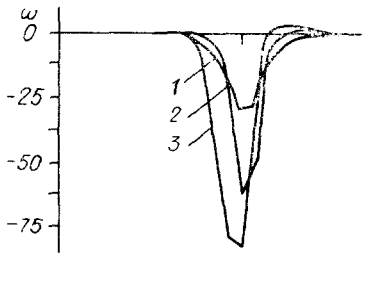


Fig. 6

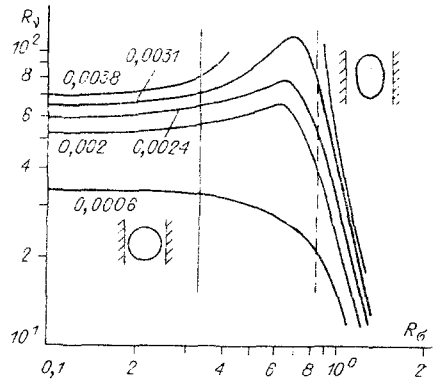


Fig. 7

for W = 0.5. The regions of the characteristic types of flows and isolines of Fr are shown in Fig. 7. On the whole their behavior is analogous to the case W = 0. The vertical lines showing regions with a definite type of deformation have shifted somewhat to the left. In the region of spherical bubbles there is a linear dependence $Fr = k_4 Re$ ($k_4 = 0.000055$). The values of Fr at the corresponding points of Fig. 7 and Fig. 9 in [6] increased approximately by a factor of three for large values of Re (where the lines Fr = const are nonmonotonic) and by a factor of 5-6 for small values of Re ($R_\nu < 5$). For large values of Re the rise velocity of the bubbles is somewhat lower than $u_0 + u_a$. In the region of spherical bubbles, where the gap between the pipe and bubble walls increases, u is somewhat higher than $u_0 + u_a$. A more accurate estimate can be obtained by comparison the diagrams for different values of W.

5. Discussion. The computational results presented in this paper carry detailed information about the structure of the fluid flows around a bubble moving in a vertical pipe and they correspond to the case when the walls determine the formation of the wake. This follows from the fact that the flows are virtually identical already at a distance of 1-1.5 units from the pipe wall. The diagrams constructed for the flow regimes make it possible to calculate the rise velocity of the bubble, the flow rate of the pumped liquid for a pipe with a given radius, and correspondingly ($\lambda$ is fixed) the size of the bubble. It is also easy to trace the general behavioral features associated with an increase of the flow rate of the fluid pumped through the pipe. Since the diagrams and the lines Fr = const have the same structure as in the case of a bubble rising in a fluid at rest [6], the dependence of the rise velocity of the bubble on $a$ will have a local maximum and as the value of $a$ approaches $R_p$ it is determined by the sum $u_0 + u_a$. For capillary tubes $R_p < \delta_\sigma = (\sigma/\rho g)^{1/2}$, since $\lambda$ is close to unity, the bubbles are virtually at rest, and the rise velocity of the bubbles is dictated by the average flow velocity. Under these conditions the bubble acts like a piston. In calculations with W = 1.5 ($\lambda = 0.8$) even for spherical bubbles the resultant of the forces acting on a bubble is directed upward – the bubble rises in a nonstationary manner.

We present another comparison, characterizing the effect of the liquid pumped through the pipe on the flow in a pipe with a fixed radius as a bubble of fixed size rises in the pipe. We take in the diagram the point with the coordinates $R_\sigma = 0.4$ and $R_\nu = 8$; this point corresponds to a liquid with $M = 1.65 \cdot 10^{-8}$. For $\lambda = 0.8$, in the case of a bubble rising in a pipe with a fluid at rest (W = 0) $Fr_0 = 0.076$ [6] (Re ≈ 13). For W = 1 we have $Fr_1 = 0.77$ (Re = 40). In both cases the bubble is approximately identically deformed and the ratio of the transverse and longitudinal dimensions as $\chi = 1.03$. We shall compare the dimensional values of $\omega$ (and the friction $\tau$) on the pipe wall. When W = 0, everywhere outside the site of the bubble $\omega$ is small and far away from the bubble $\omega$ is equal to zero. In the region of a narrow gap there is a sharp spike in $\omega$, whose maximum modulus in dimensionless form is $\omega_0 \approx 1.6$. For W = 1 outside the site of the bubble the vorticity $\omega$ assumes a positive constant value, corresponding to a Poiseuille flow, while in the region of a narrow gap the spike in $\omega$ has the modulus $\omega_1 \approx 0.47$. Since the equations were made dimensionless with respect to the rise velocity of the bubble, which has a different value in each case, we obtain the ratio of the dimensional values of $\omega'$ at the point where they are highest in modulus $\frac{\omega_1'}{\omega_0'} = \frac{\omega_1}{\omega_0}\frac{u_1}{u_0} = \frac{0.47}{1.6}\sqrt{\frac{Fr_1}{Fr_0}} \approx 0.95 < 1$. Thus, the peak of the vorticity $\omega$ (and hence the peak of $\tau$

also) does not decrease for bubbles which are only slightly deformed if the bubble rises in an upward flow. In the region of deformed bubbles ($R_\sigma = 1$, $R_\nu = 10$, for $W = 0$ the degree of deformation $\chi = 1.17$ and is somewhat higher for $W = 1$) the analogous ratio is $\omega_1'/\omega_0' \approx 1.1$. The presence of an upward flow results in an increase of the peak friction in the narrow gap between the bubble and the pipe wall. Comparisons of calculations for $\lambda = 0.98$ give the same relations for $\omega'$ in regions of spherical and deformed bubbles.

The rise velocity is $u = (gaFr)^{1/2}$. Since $R_\sigma = a/\delta_\sigma = 0.4$, then $a = 0.4\ \delta_\sigma$. The capillary constant for most liquids $\delta_\sigma \approx 0.3$ cm, and substituting it into the formula for u we obtain $u \approx 3$ cm/sec. For a deformed bubble $R_\sigma = 1$, and hence $a = 0.3$ cm and $u = 10.2$ cm/sec ($Fr = 0.36$). The average flow velocity of the pumped liquid is equal to, respectively, 1.5 and 5.1 cm/sec, and the diameter of the pipe is equal to 3 mm and 7.5 mm in the first and second cases, respectively. In order to determine the characteristics of the flow of a given liquid moving in a pipe with a given radius and a fixed flow rate as the bubble size increases, we can obtain no more than two points from the computational results presented. This is because in the method employed for making the equations dimensionless the specific liquid for which results have been obtained can be indicated only if the parameters Re, We, and Fr are known. Since one of them (Fr) is to be determined, the values cannot be obtained for a predetermined liquid. For this purpose, it is necessary either to use an algorithm developed previously based on the algorithm employed here [7] for solving the problem of a bubble rising in a specific liquid or more detailed calculations must be performed for the parameters W, $\lambda$, Re, and We and the values for the liquid of interest must be found by interpolation.

The computational results can be used for modeling flows which appear when a bubble rises in a submerged channel. Indeed, in a submerged channel (pipe) which is open at both ends and completely submerged in the liquid, as the bubble rises it pushes the liquid, so that the bubble rises in a liquid moving upward. The flow rate of the liquid in the pipe is determined by the pushing force and the friction of the liquid against the wall. For very long pipes we shall have the case of a liquid at rest ($W = 0$). As the pipe is shortened, both overflow and motion of the liquid in the pipe (flow with some W) occur. If there are several bubbles in the pipe, then the total buoyancy force will be large and a chain of bubbles can rise in a submerged pipe with a higher velocity than in the problem with a protruding end of the pipe (dead-end channel). As the calculations show, for $\lambda$ close to unity the overflow of even a small quantity of liquid through the narrow gap between the bubble and pipe walls gives rise to an enormous local resistance in the region of the bubble. For this reason, in a submerged channel liquid is forced through the channel when there are no sharp differentials of the friction at the wall, i.e., in the "piston regime of motion," realized with a definite rise velocity. According to the calculations performed, this will happen for $W > 1$. An estimate of the velocity with which the liquid is pushed can be obtained from the following considerations. The flow rate of the liquid in the gap in the case of a bubble rising in a pipe with a protruding end is known and is equal to $u_0 s$ (s is the central cross-sectional area of the bubble). This amount of liquid must flow through an annular gap, whose area is equal to $s_p - s$ ($s_p$ is the cross-sectional area of the pipe). Then the average velocity of the liquid in the gap $W_a = u_0 s/(s_p - s)$. This is approximately the average flow velocity with which the liquid should move at the inlet and outlet of the pipe in order for the "piston regime of flow" to be realized. For $\lambda = 0.98$ we have $W_a = u_0\lambda^2/(1 - \lambda^2) = 24\ u_0$ (spherical bubble). For $\lambda = 0.8$ we obtain $W_a = (16/9)u_0$ ($u_0$ can be determined from [6]). For smaller values of $\lambda$, as one can see from Fig. 2 and [6], the negative friction peaks are not so large and their contribution to the total resistance of the liquid against the pipe wall can be small. We shall estimate W for the "piston regime of flow." In this case the volume of the liquid forced through the pipe $us = u_a s_p$, and then $u_a = u\lambda^2$ or $W = 2\lambda^2$. For $\lambda = 0.8$ we have $W = 1.28$.

## LITERATURE CITED


1. V. V. Ragulin, "Contribution to the problem of flow of a viscous liquid through a bound region with a given pressure drop or head," in: Dynamics of Continuous Media: Collection of Scientific Works [in Russian], No. 27, Institute of Hydrodynamics, Siberian Branch, Academy of Sciences of the USSR (1976).
2. G. Cognet, M. Lebouche, and M. Souhar, "Utilisation des techniques electrodynamiques pour la mesure de frottement parietal dans les ecoulements diphasiques," Houille blanche, No. 5 (1978).

3. O.N. Kashinskii, B. K. Koz'menko, S. S. Kutateladze, and V. E. Nakoryakov, "Investigation of the friction stress on a wall in an upward slug flow," Zh. Prikl. Mekh. Tekh. Fiz., No. 5 (1982).
4. V. E. Nakorjakov, O. N. Kashinsky, and B. K. Kozmenko, "Experimental study of gas liquid slug flow in a small-diameter vertical pipe," Int. J. Multiphase Flow, 12, No. 3 (1986).
5. P. K. Volkov and B. G. Kuznetsov, "Numerical solution of the problem of stationary flow of a viscous liquid past a gas cavity in a pipe," ChMMSS, 13, No. 5 (1982).
6. P. K. Volkov, "Rising of gas bubble in a pipe filled with a viscous liquid," Zh. Prikl. Mekh. Tekh. Fiz., No. 6 (1989).
7. P. K. Volkov, "Algorithm for numerical solution of the problem of stationary flow in a given liquid past a bubble," in: Proceedings of the 9th All-Union School-Seminar on Numerical Methods in the Dynamics of Viscous Liquid, Institute of Heat and Mass Transfer, Siberian Branch, Academy of Sciences of the USSR, Novosibirsk (1983).

# THREE-DIMENSIONAL STRUCTURE OF FLOW IN A SUPERSONIC UNDEREXPANDED JET

V. I. Zapryagaev and A. V. Solotchin

UDC 533.6.011

Schlieren photographs of supersonic nonisobaric jets emanating from an axisymmetric nozzle into a flooded space clearly show longitudinal bands, whose origin has not been explained in the literature. Comparing the observed longitudinal bands in a jet with analogous bands arising in the case of subsonic flow past concave surfaces suggests that these phenomena are similar. The three-dimensional perturbations on concave surfaces consist of longitudinal Taylor–Goertler vortices, whose axes are parallel to the velocity vector of the undisturbed flow [1-6]. The vortices most likely form as a result of instability of the boundary layer owing to the curvature of the streamlines on the concave wall or in the region of attachment of the detached flow. The formation of vortices causes the distribution of the gas-dynamic quantities on the surfaces over which the flow moves to be nonuniform [7, 8]. It is proposed that the alternation of dark and light colored longitudinal bands in the photographs of both rarefied [9, 10] and dense [11-13] jets is caused by the development of coherent structures of the type Taylor–Goertler vortices in the flow. The presence of longitudinal vortex structures should result in nonuniformity of the distribution of gas-dynamic quantities in the jet.

The experimental investigations performed in this work are concerned with the study of this nonuniformity in a supersonic underexpanded jet.

The spatial nonuniformity was investigated by the method of photographing and measurement of the total and static pressures in the flow region lying between the suspended shock and the boundary of the jet in the so-called compressed layer [13]. For this we chose a supersonic axisymmetric jet whose Mach number in the outlet section of the nozzle is equal to $M_a = 1.5$ in the efflux regime with underexpansion ratio $n = 10$. The jet flowed out of a conical nozzle with exit diameter $d_a = 1.4 \cdot 10^{-2}$ m and aperture half-angle 8°. The Reynolds number of the jet, calculated with respect to the parameters in the outlet section of the nozzle, is $R_a \sim 10^6$. The jet setup is equipped with an IAB-451 optical system, with whose help schlieren photographs of supersonic nonisobaric jets were obtained with an exposure time $\tau = 2 \cdot 10^{-2}$ sec. The total and static pressures were measured with the help of the corresponding standard axisymmetric pressure pickups with openings $3 \cdot 10^{-4}$ m in diameter. The cylindrical static-pressure pickup had four openings, positioned at a distance of eight units from the vertex of the conical head. In order to reduce the error of measurement the angle of inclination of the pickups with respect to the axis of the jet was equal to the

Novosibirsk. Translated from Zhurnal Prikladnoi Mekhaniki i Tekhnicheskoi Fiziki, No. 4, pp. 42-47, July-August, 1991. Original article submitted March 9, 1989; revision submitted March 23, 1990.